ELSEVIER

Contents lists available at ScienceDirect

Journal of Magnetic Resonance

journal homepage: www.elsevier.com/locate/jmr



Proton-detected solution-state NMR at 14.1 T based on scalar-driven ¹³C Overhauser dynamic nuclear polarization



Murari Soundararajan ^a, Thierry Dubroca ^a, Johan van Tol ^a, Stephen Hill ^{a,c}, Lucio Frydman ^{a,b,*}, Sungsool Wi ^{a,*}

- ^a National High Magnetic Field Laboratory, Tallahassee, FL 32310, USA
- ^b Department of Chemical and Biological Physics, Weizmann Institute of Sciences, 76100001 Rehovot, Israel
- ^c Department of Physics, Florida State University, Tallahassee, FL 32306, USA

ARTICLE INFO

Article history: Received 24 July 2022 Revised 16 September 2022 Accepted 19 September 2022 Available online 23 September 2022

Keywords:
Overhauser DNP
Hyperpolarization
solution-state NMR
¹H NMR
Heteronuclear correlations

ABSTRACT

Overhauser dynamic nuclear polarization (ODNP) NMR of solutions at high fields is usually mediated by scalar couplings that polarize the nuclei of heavier, electron-rich atoms. This leaves ¹H-detected NMR outside the realm of such studies. This study presents experiments that deliver ¹H-detected NMR experiments on relatively large liquid volumes (60 \sim 100 $\mu L)$ and at high fields (14.1 T), while relying on ODNP enhancements. To this end ¹³C NMR polarizations were first enhanced by relying on a mechanism that utilizes e⁻¹³C scalar coupling interactions; the nuclear spin alignment thus achieved was then passed on to neighboring ¹H for observation, by a reverse INEPT scheme relying on one-bond |_{CH}-couplings. Such $^{13}\text{C} \rightarrow ^{1}\text{H}$ polarization transfer ported the ^{13}C ODNP gains into the ^{1}H , permitting detection at higher frequencies and with higher potential sensitivities. For a model solution of labeled ¹³CHCl₃ comixed with a nitroxide-based TEMPO derivative as polarizing agent, an ODNP enhancement factor of ca. 5x could thus be imparted to the ¹H signal. When applied to bigger organic molecules like 2-¹³Cphenylacetylene and ¹³C₈-indole, ODNP enhancements in the 1.2-3x range were obtained. Thus, although handicapped by the lower γ of the ¹³C, enhancements could be imparted on the ¹H thermal acquisitions in all cases. We also find that conventional $^{1}H^{-13}C$ nuclear Overhauser enhancements (NOEs) are largely absent in these solutions due to the presence of co-dissolved radicals, adding negligible gains and playing negligible roles on the scalar $e^- \rightarrow {}^{13}C$ ODNP transfer. Potential rationalizations of these effects as well as extensions of these experiments, are briefly discussed.

© 2022 Elsevier Inc. All rights reserved.

1. Introduction

NMR is a powerful analytical tool to investigate the structure and dynamics of molecules in solutions. Despite its advantages, NMR suffers from an intrinsically poor sensitivity reflecting weak magnetic interactions that lead to small spin polarizations and, sometimes, from a low natural abundance of the NMR active nucleus of interest. Dynamic Nuclear Polarization (DNP) is an effective and versatile technique that can be used to increase NMR's sensitivity; DNP takes advantage of an electron's large gyromagnetic ratio, and transfers its intrinsically larger polarization to nuclei for their NMR investigation [1–2]. However, while the high efficiencies of electron → nucleus polarization transfer mechanisms at cryogenic temperatures have enabled DNP to revolution

E-mail addresses: lucio.frydman@weizmann.ac.il (L. Frydman), lucio.frydman@weizmann.ac.il, sungsool@magnet.fsu.edu (S. Wi).

ize solids and in vivo metabolic NMR [3-13], solution-state NMR has not seen comparable successes yet - particularly when executed at the high magnetic fields of interest in analytical spectroscopy. Liquid state DNP operates primarily through the Overhauser DNP (ODNP) mechanism, whereby a free radical dissolved in solution exhibits fluctuating interactions between the paramagnetic electrons and the target nuclei under NMR investigation [14]. When the electron spin polarization is perturbed away from equilibrium, for instance by the continuous application of microwave (MW) irradiation at its Larmor frequency, these timedependent interactions lead to a cross-relaxation between the electron and the coupled nuclei of interest, eventually transferring the electron spin polarization to the nucleus [15]. The extent of this ODNP enhancement will depend on both the degree of saturation imparted on the electron spin resonance (ESR) line, and on the efficiency of the electron/nuclear cross-relaxation. These processes can become significantly inefficient as the targeted solution is studied in increasing magnetic fields. On the hardware side, the main obstacle to high-field solution-state ODNP is the requirement

^{*} Corresponding authors.

for ever higher MW powers for saturating the ESR line(s): a typical sample, prepared based on nitroxides as ODNP polarizing agents, will require ~ 0.2 mT B₁ fields to achieve this saturation at high fields [16]. Reaching such B₁ values requires the use of microwave resonant cavities [17-18], or high power sources such as gyrotrons [19-21]. Resonant cavities overcome the necessity of using a high MW power, but restrict the sample volumes to sub-microliter ranges and add significant complexity to the radiofrequency (RF) resonator design, making it difficult to integrate multiple RF channels while maintaining a high efficiency [22-23]. On the other hand, the use of high powers may enable the utilization of a conventional liquid-state NMR probe-head that allows the use of a large sample volume. However, unless special provisions are taken, this method cannot avoid inducing substantial sample heating [24]. An even more fundamental challenge is posed by the lack of efficiency of the electron-nucleus cross-relaxation at high magnetic fields [25]. Improving this requires tailoring the solution state dynamics to match ever shorter time scales, demanding for instance the use of supercritical fluids as low-viscosity solvent media [19,26]. Alternatively, an ODNP-efficient cross relaxation can be found in radical-target combinations where the free electron is effectively coupled to specific nuclear sites on the target molecule via contact hyperfine interactions [17-31]. While strongly site-specific, the ODNP mechanism that relies on this e⁻nucleus contact hyperfine interaction has been shown to remain significant even at high magnetic fields [17,20,23,30-31]. This mechanism is based on scalar interactions that require significant electron densities localized, albeit transiently, in the polarized nucleus. Because of this, scalar ODNP enhancements have been reported for heavier species such as ¹³C, ³¹P, ¹⁹F and ¹⁵N [17,20,24,27], but leaves outside their realm ¹Hs, the species with highest intrinsic sensitivity out of all conventionally observed NMR nuclei.

This situation is not exclusive to scalar-based solution-state ODNP: Numerous hyperpolarization methods have emerged, where ¹⁵N or ¹³C species can be efficiently polarized, but ¹H counterparts will either not polarize or not maintain their polarization sufficiently long for enabling meaningful measurements. Given the advantages resulting from relying on the bigger gyromagnetic ratio of ¹Hs, a number of experiments have been recently reported whereby dissolution DNP [32-35], CIDNP [36], or PHIP/PASADENA [37] experiments, are complemented for transfers to ¹H for an enhanced detection. These transfers could happen spontaneously [38] or, more commonly, via $I(^{15}N^{-1}H)$ - or $I(^{13}C^{-1}H)$ -based polarization transfers [39-41], leading to an additional gain in sensitivity and occasionally in resolution as well [32-38]. This work is based on a similar concept, but for polarization enhancements that rely on scalar-driven ODNP on ¹³C species on large volumes and at high fields. These experiments are demonstrated on model solutions containing ¹³CHCl₃, 2-¹³C-phenylacetylene and ¹³C₈-indole, which are enhanced by ODNP using TEMPO as the polarizing radical. When passing this ODNP-enhanced ¹³C polarization to directly bonded ¹Hs by reverse insensitive nuclei enhanced by polarization transfer (rINEPT) schemes, signal increases of ca. 5-fold are achieved on the ¹H spectrum when compared with microwaveless acquisitions. Double-resonance investigations also clarify the role of the protons in the $e^- \rightarrow {}^{13}C$ DNP transfers. These approaches make a suitable starting point to exploit ODNP enhancements on ¹H NMR, as well as to build 2D liquid-state NMR experiments at high magnetic fields. It is worth remarking that while this study was undergoing peer review, a similar study relying on hardware developed for solid state DNP NMR at 400 MHz and smaller samples was reported by Rao et al. [50].

2. Experimental details

ODNP NMR experiments were performed in a 14.1 T Oxford magnet interfaced to a Tecmag Redstone NMR console configured for ¹H operation at 600 MHz. A Bruker-CPI second-harmonic 395 GHz gyrotron was used as a high-power MW source, with a quasi-optical bench to control beam power and polarization, and a shutter to rapidly switch the MW irradiation on and off [24]. The MW power used in all ODNP experiments presented in this work was 13 W. The probe used in the experiments is based on a Varian HX 600 MHz direct-detect broadband 5 mm solution state NMR probe, modified with a customized sweep coil for targeting various radicals, as described in a previous publication [27]. The probe was fitted with a smooth-walled microwave waveguide that replaced the probe's original glass Dewar (Fig. 1a), and ended up at the coil deck with a custom-designed spline-profile horn, shining a TE11 mode MW beam with a 3 mm diameter directely at the sample located inside the NMR coils. Unlike an earlier design were this "sample-waveguide" completely enclosed the sample tube throughout the working length of the NMR coils, [27] the new design uses the sample and sample tube as a dielectric waveguide to contain the MW beam (Fig. 1b), Just below the sample, the TE11 mode waveguide was cut horizontally with multiple slots with a spacing optimized to increase the efficiency of the radiofrequency irradiation at the sample while minimizing the MW transmission losses at 395 GHz. These slots also serve as a path for flowing a stream of nitrogen gas to cool the sample, delivered from the bottom of the probe through the MW waveguide, thus helping to reduce the microwave heating. This design allows us to simultaneously tune both RF channels (${}^{1}H$ and X, where X = ${}^{31}P$, ${}^{13}C$ or ${}^{15}N$) for double resonance experiments, while allowing an efficient microwave irradiation on the sample. The sample tube is made of fluorinated ethylene propylene (FEP), a material transparent to microwaves. The index of refraction of FEP is about 1.5 [42], similar to that of typical NMR solvents; this index is larger than that of the surrounding air (\approx 1), allowing the sample-FEP tube combination to act as a dielectric waveguide for the microwaves. A MW nutation measurement using an in-situ pulsed EPR spectrometer on the same setup [27], yielded a peak MW magnetic field of 4.75 μT (133 kHz) with a 7 mW source power, corresponding to a B_1 \approx 0.2 mT (5.6 MHz nutation frequency) at the gyrotron-supplied MW power. Figs. 1c, 1d show ¹³C and ¹H nutation curves measured using this custom-designed double-resonance ODNP NMR probe; well-defined 10 us and 24 us 90° excitation pulses were exhibited for the ¹³C and ¹H channels for ca. 120 and 50 W RF powers, respectively. Based on these nutation behaviors we estimate 8 % and 14 % deviations $(I_{9\pi/2}/I_{\pi/2} = 0.92 \text{ and } 0.86, \text{ respectively})$ [47] in the RF homogeneity over the full sample for the ¹³C and ¹H channels, respectively, confirming essentially no disturbances from the waveguide components or the sweep coil, on the RF performance of the probe.

Sample solutions containing a variety of target molecules $^{-13}\text{CCl}_4$, $^{13}\text{CHCl}_3$, $2^{-13}\text{C-phenylacetylene}$ and $^{13}\text{C}_8$ -indole– were chosen to examine the ODNP-driven ^{13}C signal enhancements. These compounds probe the $e^- \rightarrow ^{13}\text{C}$ ODNP phenomenon on $^{1}\text{H}-^{13}\text{C}$ moieties with sp^3 , sp^2 and sp hybridizations, all of which have been shown to exhibit ^{13}C NMR enhancements as driven scalar ODNP. [23,29,43–45] The sample solutions formulated for the DNP experiments were as follows: (1) a mixture of 2 % v/v $^{13}\text{CHCl}_3$, 8 % v/v $^{13}\text{CCl}_4$ and 10 mM 2,2,6,6 tetramethylpiperidinyloxy (TEMPO) radical in 100 μ L hexane-d₁₄; (2) a solution of 0.32 M 2- $^{13}\text{C-phenylacetylene}$ and 10 mM TEMPO in 60 μ L n-heptane-d₁₆/toluene d₈ (v/v = 3/1); (3) a solution of 0.44 M $^{13}\text{C}_8$ -indole

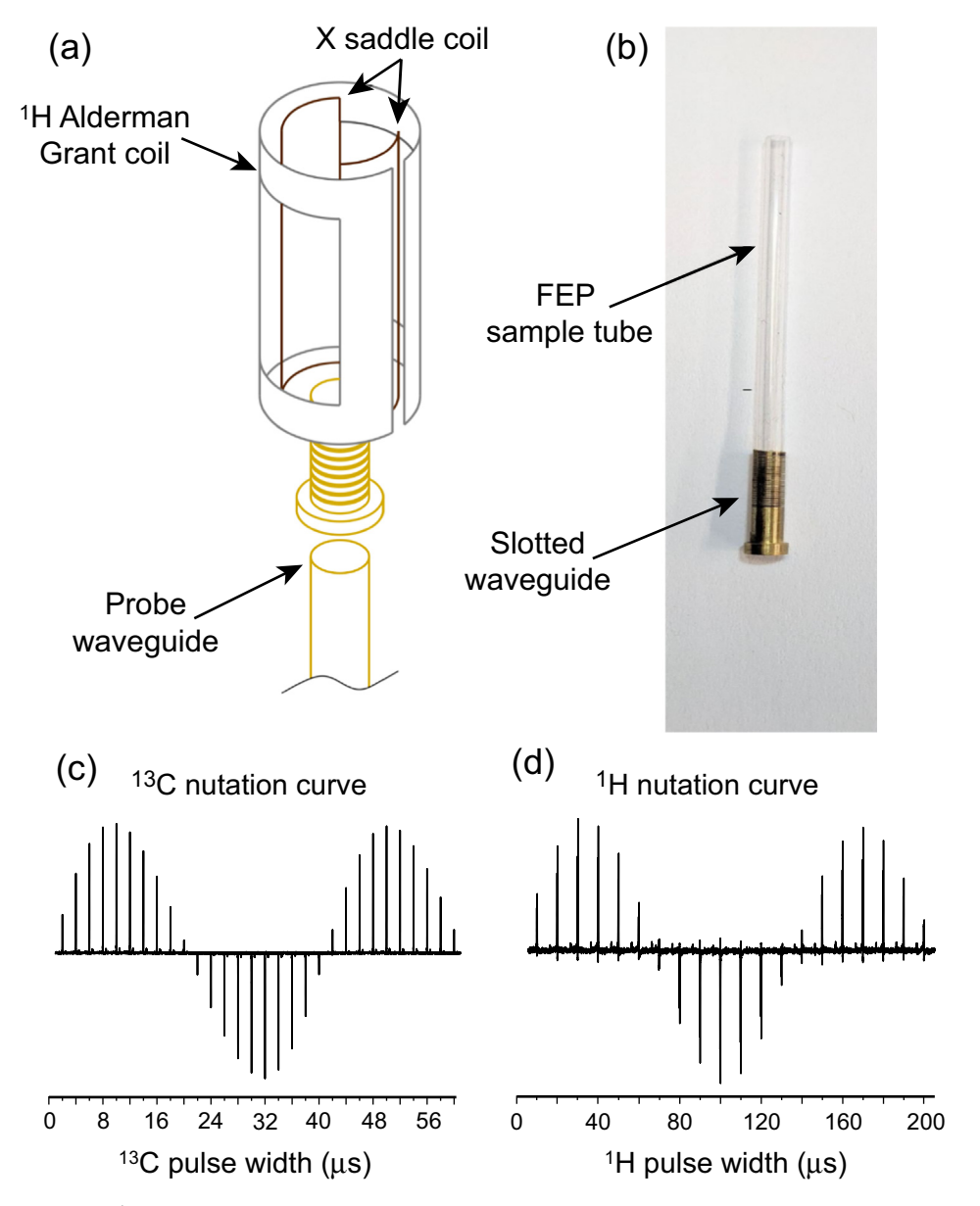


Fig. 1. (a) Schematic of the customized ¹H-X double-resonance ODNP NMR probe-head used in this work, highlighting the smooth-walled probe waveguide used to channel the Gyrotron beam to the sample, the slotted waveguide, and the RF coils. During DNP the samples are cooled by a nitrogen gas stream flowing through the waveguide. (b) Slotted waveguide with FEP sample tube partially inserted into it; during experiments the FEP tube sits inside the 2.5 cm long NMR coils. (c, d) ¹³C and ¹H nutation measurements carried out on a sample of 25 % ¹³CHCl₃ and 10 mM TEMPO in ¹³CCl₄, using the double-resonance ODNP probe.

and 10 mM TEMPO in 60 μ L n-heptane- d_{16}/p -xylene- d_{10} (v/ v = 4/1). All these solutions were based on non-polar solvents such as hexane and heptane that are relatively transparent to microwaves; a minimum amount of toluene or p-xylene was added as an auxiliary solvent to ensure the solubility of phenylacetylene and indole, respectively. All these compounds were purchased from Sigma-Aldrich and used as purchased. These sample solutions were pipetted into 3 mm OD / 2 mm ID FEP tubes for the experiments, that were either welded shut or closed with a Teflon cap for the DNP NMR experiments. All solutions were deoxygenated by performing 5 freeze-pump-thaw cycles under Ar gas environment before preparation; additionally, the filled sample tubes were stored in a glove box for 2 or 3 days under an Ar environment to allow any dissolved oxygen to diffuse out of the solution; the cooling nitrogen gas (vide supra) prevented any oxygenation during the experiments themselves. The 10 mM TEMPO concentration used in these tests came out of a series of optimization studies,

where the efficiency of the scalar ODNP was high enough to allow us relatively short MW CW irradiation times (thereby limiting MW-induced heating), while leaving a long enough nuclear T_1 time to enable an efficient polarization. Radical concentrations were verified using a Bruker EMXnano EPR spectrometer before carrying out the ODNP experiments.

Fig. 2 shows the NMR pulse sequences used in this work. Directly polarized 13 C or 1 H NMR spectra were acquired using a single 90° pulse or a 90° – τ - 180° – τ Hahn echo sequence (to eliminate a ca. 10 µs ringdown time ascribed to the presence of the metallic waveguide and potential 1 H or 13 C background signals), with or without 1 H or 13 C decoupling (Fig. 2a). WALTZ-16 [46] was used as 1 H- or 13 C-decoupling sequences; 4.5 kHz nutation fields were used for 1 H decoupling and 7.1 kHz for 13 C. The e⁻- 13 C ODNP effect was initiated by turning on the MW irradiation for a time d_2 before applying the RF pulses. To limit sample heating, the gyrotron beam was gated "on" using a mechanical shutter over

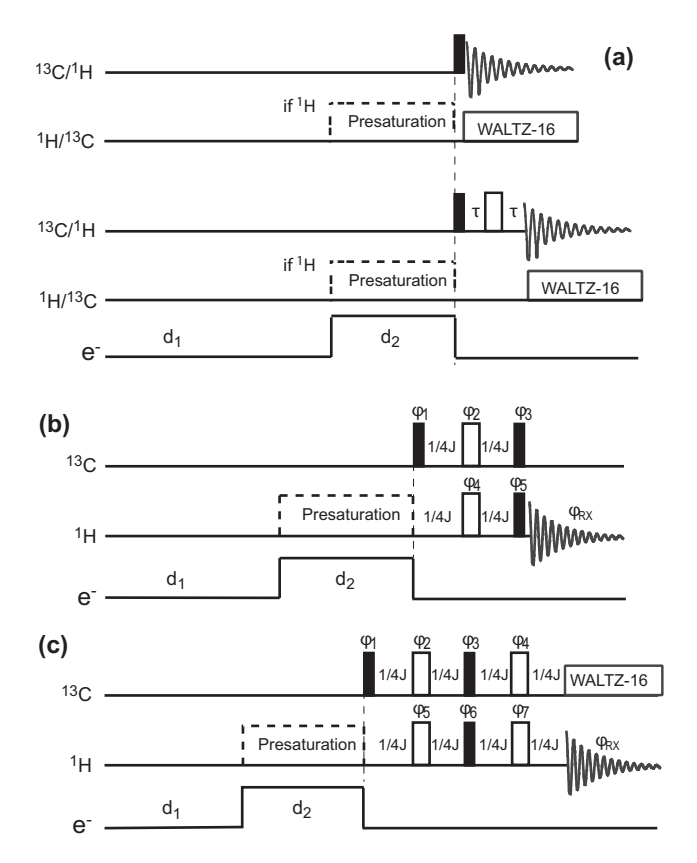


Fig. 2. ODNP NMR pulse sequences employed in this study. Black rectangular bars represent 90° pulses, and empty rectangular bars represent 180° pulses. Microwave gating was turned on for a delay time d_2 prior to the application of RF pulse(s), and turned off for all other periods including d_1 , acting as recycling delay. A 1 H presaturation pulse was sometimes applied prior to the 90° 13 C excitation pulse for probing a putative NOE enhancement of the signals. Shown are pulse sequences for (a) direct 13 C observation with 1 H decoupling (with or without spin-echo); (b,c) indirect 14 H observation via a 13 C $^{-1}$ H rINEPT signal transfer. Shown in (c) is the refocused 13 C $^{-1}$ H rINEPT sequence with 13 C decoupling. Delays in (b,c) were tuned to 14 J(13 C $^{-1}$ H). Phase cycling: (b) ϕ_1 =(x)8,(-x)8; ϕ_2 = ϕ_4 = x,-x; ϕ_3 =(x)4,(y)4,(-x)4, (-y)4; ϕ_5 = y,y,-y,-y; ϕ_{Rx} = x,x,-x,-x,y,y,-y,-y. Phase cycling in (c) ϕ_1 =(x)8,(-x)8; ϕ_2 = ϕ_4 = ϕ_5 = x,-x; ϕ_3 = y,y,-y,-y; ϕ_6 =(x)4,(y)4,(-x)4,(-y)4; ϕ_7 =(x,-x)2,(y,-y)2; ϕ_{Rx} = x, x,-x,-x,-y,y,-y,-y.

typical d_2 times of 1 to 2 s prior to the application of any NMR pulse; this gate was turned "off" during the RF pulses, the signal acquisition period, and the recycling delay time d_1 (5 to 20 s). The "on" MW irradiation time was adjusted based on the T_1 relaxation time of the polarized nuclei, while the d_1 time was chosen relatively long in order to minimize sample heating. In all cases presented here, peak broadening or shifting due to excessive heat absorption did not occur under any condition. ¹H presaturation with a 10 kHz RF field was occasionally applied to examine the potential presence of $^1H_-^{13}C$ nuclear Overhauser enhancement (NOE) effects. The ^{13}C signals enhanced by ODNP were also observed indirectly via J-coupling mediated rINEPT $^{13}C_-^{1}H$ sequences (Fig. 2b and 2c), whose echo times were adjusted to $1/4J(^1H_-^{13}C)$.

3. Results

Before discussing the potential of $^{13}\text{C} \rightarrow ^{1}\text{H}$ transfers under ODNP, we consider it worth examining the extent of the conventional $\{^{1}\text{H}\}^{-13}\text{C}$ NOE effect. 4 % $^{13}\text{CHCl}_{3}$ solutions in CDCl₃ with and without 10 mM TEMPO were thus treated with identical cycles of freeze–pump-thaw deoxygenation, and the NOE effect examined under Ar gas environments. In the absence of TEMPO a $\{^{1}\text{H}\}^{-13}\text{C}$

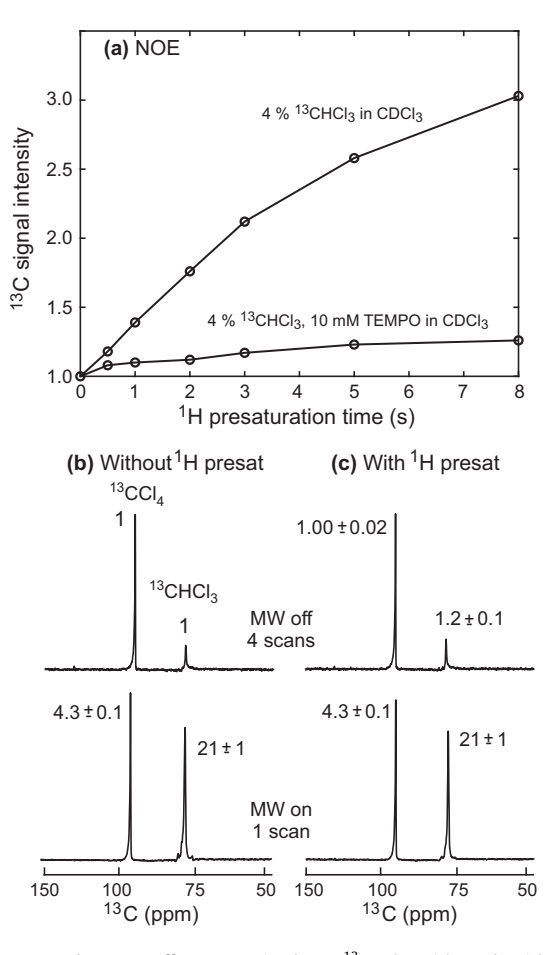
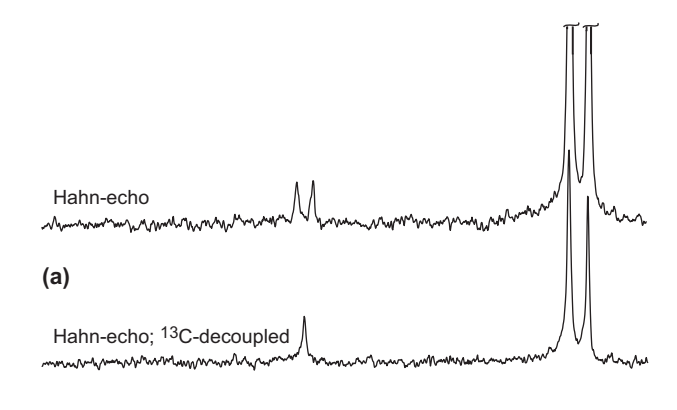


Fig. 3. NOE and ODNP effects examined on 13 CHCl₃ with and without 1 H presaturation / MW irradiation. (a) NOE effects measured on 4 % 13 CHCl₃ in CDCl₃ with and without adding 10 mM TEMPO. (b,c): 13 C NMR spectra obtained on 2 % 13 CHCl₃, 8 % 13 CCl₄, and 10 mM TEMPO in 100 μL hexane-d₁₄ without (b) and with (c) 1 H presaturation while turning "off" (center) or "on" (bottom) the MW irradiation. The "off" spectra were acquired with 4 scans and the "on" spectra with 1 scan. Signal enhancement factors were estimated with respect to the "off" spectrum without 1 H presaturation (areas for each resonance set to 1). The ppm scale was calibrated using the 13 CHCl₃ peak (77 ppm), measured with 1 H decoupling and without microwaves on a TEMPO-free sample.

NOE signal enhancement factor of 3 was observed after \approx 8 s 1 H presaturation, which is the theoretically expected value [48]: η = $(I-I_0)/I_0 \approx 3$, where I and I_0 are signal intensities measured with and without ¹H presaturation, respectively. However, in the presence of 10 mM TEMPO, the NOE effect was greatly reduced, leaving a residual enhancement of 1.2 (Fig. 3a), with everything else being equal. Fig. 3b and Fig. 3c, respectively, show ¹³C NMR spectra acquired on this TEMPO-containing sample with and without ¹H presaturation, under thermal equilibrium and under ODNPenhanced conditions. Upon irradiating the sample with microwaves at 395 GHz both the 13CCl₄ and 13CHCl₃ signals were enhanced, with ODNP enhancement factors $\epsilon \approx 4.3 \pm 0.1$ and 21 ± 1, respectively (enhancements were always calculated using areas of the integrated peaks). As reported in the literature the ¹³-CHCl₃ carbon, possessing a directly-bonded ¹H, displays an ODNP enhancement that is significantly greater than that of the protonless ¹³CCl₄ -apparently because the ¹H enables a hydrogen-bondlike connection with the radical facilitating the e⁻¹³C scalar coupling interaction [44–45]. As also shown in Fig. 3, the ODNP signal enhancement detected for the chloroform ¹³C remains at about 21 (for 13 W MW powers and $d_2 = 2$ s) regardless of the presence or absence of ¹H presaturation. This confirms that the ¹H-¹³C cross relaxation, which is a mutual process, can be disregarded when



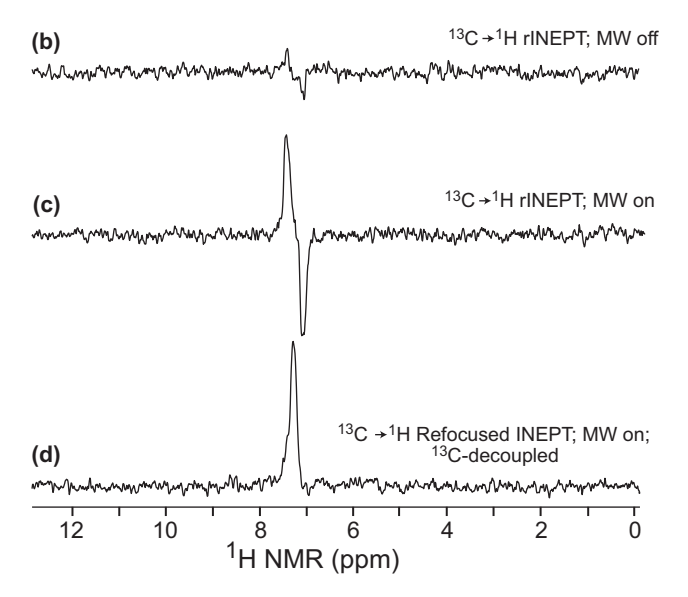


Fig. 4. ¹H NMR spectra measured on a ¹³CCl₄/¹³CHCl₃ in the same hexane-d₁₄ solution as used in Fig. 3. (a) Thermally polarized ¹H spectra with ¹³C WALTZ-16 decoupling; peaks at 1-2 ppm arise from residual hexane ¹Hs. (b-d) ¹H signals transferred from the ¹³C in ¹³CHCl₃ upon utilizing ¹³C \rightarrow ¹H rINEPT (Fig. 2b and 2c) without (b) and with (c, d) microwave irradiation. 16 scans were used in every case. The 1/4J(¹H-¹³C) delay time used in the rINEPT sequence was set for J (¹H-¹³C) = 130 Hz.

the targeted molecule is comixed in solution with ≈ 10 mM of a radical acting as much more efficient relaxation sink.

Fig. 4 illustrates the outcome of applying the various sequences illustrated in Fig. 2 on the ¹³CHCl₃/¹³CCl₄ solution, when focusing on ¹H NMR acquisitions. Shown on top as an initial reference are thermally polarized ¹H NMR spectra acquired with and without ¹³C decoupling (Fig. 4a). These ¹H signals showed some broadening but virtually no change in intensity upon MW irradiation, reflecting the unfavorable coupling of TEMPO to protons at high fields³⁰ and the absence of meaningful e⁻¹H DNP interactions (spectra not shown). Applying the rINEPT sequence on this ¹³C-labeled solution cleans up the residual solvent resonances in the 1-2 ppm region, but imparts a significant sensitivity penalty by virtue of the ¹³C's lower thermal polarization under these conditions (Fig. 4b). By contrast, when relying on the ¹³C ODNP enhancement, the indirectly-polarized ¹H can be obtained with a significant sensitivity enhancement vs its thermal counterpart, via a $^{13}\text{C} \rightarrow ^{1}\text{H}$ rINEPT block (Fig. 4c); a slightly larger ¹H enhancement is observed when employing the refocused INEPT scheme and ¹³C decoupling, even if the longer time required by this module robs the decoupling from its full potential: the ideal sensitivity of the refocused ¹³C-decoupled rINEPT in Fig. 4d should be twice that observed in Fig. 4c, while the actual enhancement is only \approx 1.5x. This reflects

in part the relatively short 1 H $_{2}$ of this radical-doped chloroform sample. Still, the ODNP enhancement factor observed in these 1 H-detected experiment was ca. 5x when compared with the 1 H thermal acquisition, and ca. 20x when compared with the rINEPT 1 H spectrum obtained if starting from thermal 13 C polarization. Considering that the gyromagnetic ratios of 13 C and 1 H differ by a factor of 4 these observed enhancement factors are reasonable, and indicate a good efficiency for the 13 C \rightarrow 1 H rINEPT transfer.

Fig. 5 presents a similar series of e⁻¹³C⁻¹H scalar-coupling ODNP NMR experiments, performed on a 0.32 M 2-13Cphenylacetylene, 10 mM TEMPO solution in 60 µL heptane d_{18} /toluene d_8 (v/v = 3/1) (this amount of toluene d_8 added to better solubilize phenylacetylene in heptane-d₁₆). As in the chloroform case this sample was deoxygenated by freeze-pump-thaw under Ar, and kept in a N_2 gas stream (precooled to -20 °C) during the ODNP experiments. Also as in the chloroform case, the NOE effect arising on the ¹³C upon presaturating ¹Hs in this sample was much below the maximum theoretical value: about a 1.3x enhancement was detected, both when observing 13C directly and when observing the signal transferred to ¹H from the ¹³C following a rINEPT module (Fig. 5a/5b and 5f/5g). ¹³C ODNP enhancement on the C2 of this molecule was $\approx 10.5x$, and varied negligibly within the margin of error (estimated from 3 independent measurements) and/or if adding ¹H NOE by presaturation to the MW irradiation (Fig. 5c, 5d). MW irradiation again had no effect on the ¹H NMR spectrum of this solution, but ¹H spectra monitoring the ¹³C ODNP effect indirectly via rINEPT transfers (Fig. 5h/5i) showed a 9x increase vs MW-free acquisitions. These ODNP enhancements were identical regardless of whether ¹H presaturation was or was not used, and amounted to a ca. 2x gain in the ¹H signal sensitivity when compared to the thermal ¹H spectrum (Fig. 5e with ¹³C decoupling). This observation is again consistent with the ODNP enhancements observed for ^{13}C , as $\epsilon\approx$ 10.5 $\gamma_\text{C}/$ $\gamma_\text{H}\approx$ 2.6 would be the maximum possible ¹H enhancement, with the difference probably reflecting losses over the course of the transfer.

Fig. 6 presents a final example of ¹³C- and ¹H-detected ODNP NMR experiments, measured on a 0.44 M ¹³C₈-indole and 10 mM TEMPO solution in 60 μ L heptane- d_{16}/p -xylene- d_{10} (v/v = 4/1). As all carbons in this compound were labeled, a variety of enhancements can be seen in this sample -even if at the price of having multiple homonuclear J_{C-C} couplings complicating the spectra. As in the previous cases, the {¹H}-¹³C NOE enhancements upon ¹H presaturation are relatively modest, ranging from none for quaternary carbon C9, to ca. 1.4x for methine carbon C6. Site-specific enhancements are also a feature of the ODNP-enhanced ¹³C NMR, with gains ranging from $\approx 1x$ for C9, to $\approx 3x$ for methine carbons C3 and C6. Once again, addition of a $\{^1H\}^{-13}C$ NOE effect does not add significantly to these e⁻→¹³C ODNP enhancements, with marginal enhancements adding to the ODNP upon turning on a concurrent ¹H presaturation. All these site-specific signal enhancements are transferred in a nearly one-to-one fashion upon indirectly observing them on the ¹H NMR spectra, receiving the individual ¹³C polarizations via rINEPT transfers from their directly-bonded neighbours (Fig. 6, right-hand column).

4. Discussion and conclusions

The present study explored the effects of heteronuclear NOEs and of scalar-coupling-mediated ODNP ^{13}C polarization enhancements, on organic solutions of several compounds ($^{13}\text{CHCl}_3$, 2^{-13}C -phenylacetylene, $^{13}\text{C}_8$ -indole) codissolved with TEMPO. The potential of transferring these enhanced ^{13}C signals to ^{1}Hs for final detection with the aid of rINEPT-based experiments, was also explored. These experiment require a custom-designed solution-state $^{1}\text{H}_{-}^{13}\text{C}_{-}$ electron multiple-resonance DNP setup, capable of

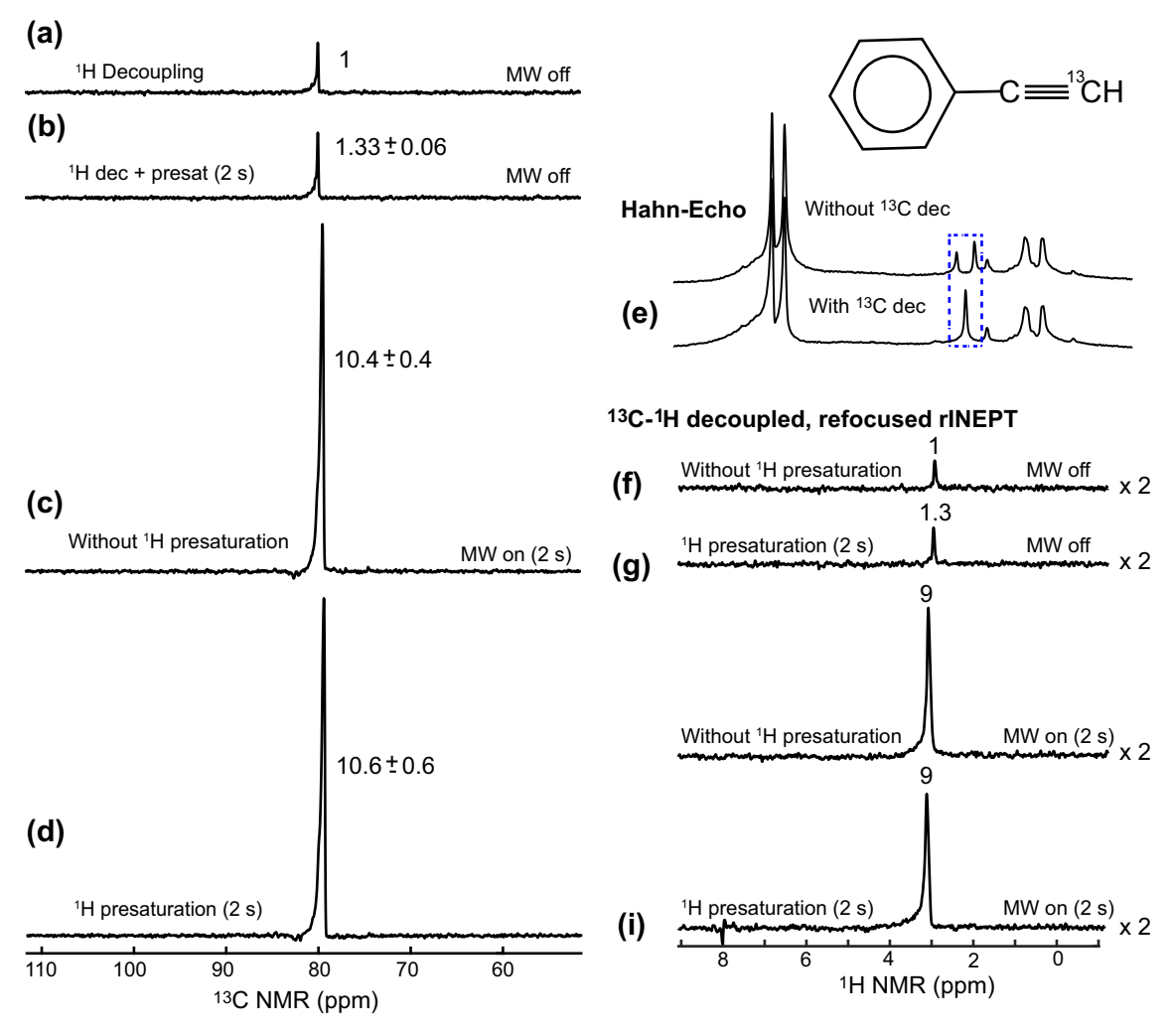


Fig. 5. 13 C (a-d) and 1 H (e-i) NMR data measured for a 2- 13 C-phenylacetylene, 10 mM TEMPO in 60 μL heptane/toluene solutions under a variety of NOE (1 H presaturation) and e $^{-}$ \rightarrow 13 C ODNP conditions, as specified in each panel. Shown in panels (f-i) are reversed INEPT 1 H spectra acquired assuming a J(1 H- 13 C) = 240 Hz. All spectra were acquired by co-adding 16 scans for signal averaging with d₁ = 20 s; all ppm scales were adjusted according to the literature data [43]. Full-widths at half-heights (FWHH) for the 13 C with and without MW irradiation were 23 Hz and 70 Hz, respectively; those for 1 H with and without MW were 31 Hz and 36 Hz, respectively. Note that different receiver gain factors were used in measuring the 1 H spectra: gain for (e) was twice as for (f-i). Numbers indicate relative peak areas stemming from taking thermal 13 C/ 1 H { 1 H/ 13 C}-decoupled intensities of unity.

delivering quality RF pulses and intense MW fields, without compromising on the abilities of the solution NMR acquisitions. Further, these acquisitions were assayed using relatively large (60 \sim 100 μL) sample volumes, while operating at high magnetic fields (14.1 T) of analytical interest. As a result of all these demands, the ODNP enhancements reported in this study were not as high as they could be: for instance in our previous publication, employing nearly the same setup and this study, [24] $e^- \rightarrow {}^{13}C$ ODNP enhancements of up to \sim 80 were reported for 13 CHCl₃ -as opposed to the ≈20x enhancement reported here. The previous study, however, used higher MW powers and longer MW irradiation times; these conditions caused heating and temperature gradients in the sample, leading to substantial peak broadening and a significant loss in spectral resolution [24]. Such broadenings would have made meaningless the acquisition of ¹H NMR data. characterized as they are by a much narrower ppm range than its heteronuclear counterpart. A sweet spot was therefore sought where good resolution and significant ODNP enhancements, could be simultaneously achieved. The experimental results shown in Figs. 3-6 evidence such achievements, with ¹H-decoupled ¹³C FWHHs increasing by under 50 % and showing negligible chemical shift displacements after 2 s of ≈ 5 W ¹H irradiation concurrent with

a ≈13 W MW irradiation. Larger ODNP enhancements (as measured by peak areas) could have been achieved if extending these irradiation times, yet the resolution of the ensuing spectra would have suffered unless extending even further the already long recycle delays used in this study. This would in turn compromise the sensitivity/unit_time performance of ODNP NMR; additional improvements in MW heating management are thus in progress in order to reap the full benefits of higher MW-driven enhancements. It is worth pointing out that temperature-gradient-driven NMR line broadenings are not uniform, and vary from compound to compound (e.g., chloroform's ¹³C peak position is more sensitive to temperature than tetrachloromethane's) as well as from nucleus to nucleus. Hence, the acceptable degree of sample heating will vary depending on the specifics of the application. Also important to remark is the role of the solvent, whose dielectric losses will be the main determinants of the MW heating arising in large-volume DNP experiments; for instance, the experiments that were demonstrated here using essentially apolar solvents, would be impossible in absorbing solvents such as water, both because of sample heating and of limited MW penetration.

With these 13 C enhancements achieved, rINEPT-based 13 C \rightarrow 1 H transfers were explored to port ODNP's polarization gains to the

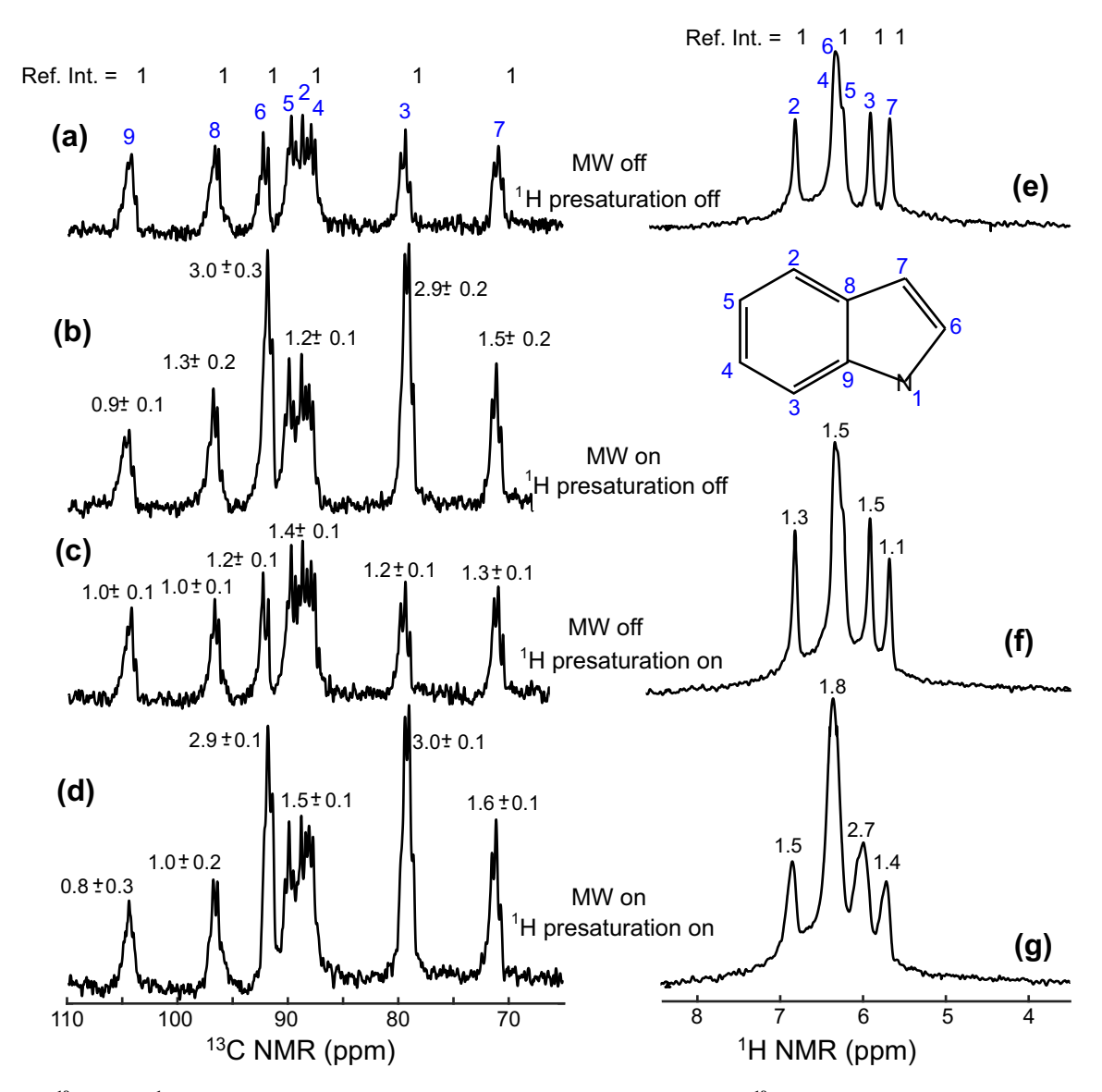


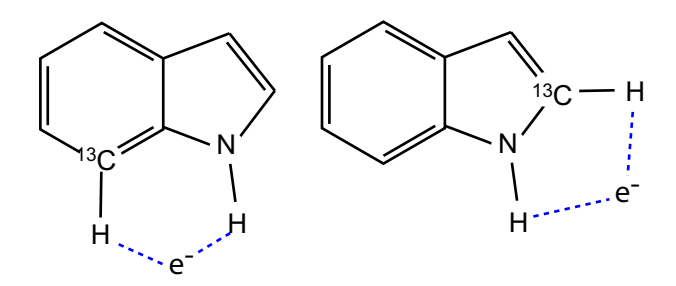
Fig. 6. Summary of 13 C (a-d) and 1 H (e-g) standard, NOE- and ODNP-enhanced NMR results measured on a 0.44 M 13 C₈-indole, 10 mM TEMPO sample in 60 μ L heptane-d₁₆/p-xylene-d₁₀(v/v = 4/1). All 13 C (left) and rINEPT 1 H (right column) spectra were taken with 1 H and 13 C decoupling, respectively. 1 H presaturation and MW irradiation were used as indicated; also indicated are the assignments of the peaks to the different sites in the molecule (labeled in the inset structure) and the relative intensities of the peaks vs heteronuclear-decoupled, thermal acquisition counterparts. Each 13 C / 1 H spectrum coadded 64 / 16 scans, respectively. 1 d and 1 d times used (cf. Fig. 2) were 5 and 2 s, respectively. The delay time 1 4J(1 H- 13 C) used in the rINEPT sequences leading to the spectra in the right-hand column was determined by J(1 H- 13 C) = 160 Hz. The chemical shifts of the 12 C and 14 H peaks were calibrated according to literature values [49]. Upon applying MW, the FWHH for the heteronuclear decoupled 1 H and 13 C peaks changed on average from 26 to 33 Hz and from 40 to 80 Hz, respectively.

more sensitive 1H species. Such an approach is inherently of limited efficiency due to its reliance on transferring from a low- to a high- γ nucleus, yet it presents advantages and opportunities previously demonstrated for dissolution DNP methods –also a class of experiments feasible mostly on low-gamma nuclei. The signal increases that could then be observed in the 1H spectra were near the expected maxima, and in all cases served to enhance the proton signals over their thermal counterparts. Further investigations are in progress to explore further uses of the ODNP enhancements achievable in these heteronuclear experiments, particularly in connection to extensions of ODNP-enhanced NMR to 2D heteronuclear correlations.

Another aspect explored in these multinuclear studies concerns the role of the ¹Hs and, in particular, of a concurrent ¹H saturation upon executing ODNP, on the polarization enhancement achieved by the ¹³C. On thermal samples it was observed that the addition of a TEMPO radical (10 mM) to the solution under study, quenched

the full-sized one-bond NOE effects that were otherwise present in a radical-free, deoxygenated counterpart. This is to a large degree expected, given the substantial paramagnetic relaxation competition brought about by the addition of the free radical –particularly of a free radical that will interact with the ^{13}C to later lead to an ODNP enhancement [23]. Interestingly, the ODNP enhancement changed negligibly upon concomitantly irradiating the ^{1}H that is in principle also involved in the formation of the transient species enabling the scalar-driven enhancement. This lends credence to the claim that the ^{1}H nucleus plays little or no significant role in facilitating the $e^- \rightarrow ^{13}\text{C}$ polarization transfer, and that this is dependent on direct electron radical spin density positioning at the carbon nucleus.

A final topic worth discussing concerns the roles that different moieties play in enabling the $e^- \rightarrow {}^{13}\text{C}$ scalar interaction. It is speculated that protons attract radical electrons by forming a hydrogen-bonding-like interaction, thereby aiding to a closer con-



Scheme 1.

tact between the electron and ¹³Cs [23,28,31]. This is consistent with the observation (Fig. 3) that ¹³CHCl₃, which contains a ¹H, shows a superior e⁻¹³C ODNP enhancement effect than ¹³CCl₄ that does not contain any hydrogen. It is also consistent with the sites C3 and C6 showing the largest enhancements in indole (Fig. 6). These ¹³C-¹Hs would be under favorable conditions for forming an e⁻¹³C scalar coupling interaction by creating five- or six-membered ring complexes with the TEMPO radical electron; the hydrogen-bonding-like connections in these hypothetical rings could lead to ²J(e⁻¹³C)-type scalar couplings (Scheme 1) favoring the ODNP. It is interesting to note, however, that despite being the closest ¹³C from the amine group the quaternary site C9 does not show any noticeable e⁻¹³C ODNP enhancement, remarking again the importance of having a hydrogen-bond-like structure in enabling these effects.

Data availability

Data will be made available on request.

Declaration of Competing Interest

The authors declare that they have no known competing financial interests or personal relationships that could have appeared to influence the work reported in this paper.

Acknowledgment

This work was performed at the National High Magnetic Field Laboratory, which is supported by the National Science Foundation (NSF) Cooperative Agreement No. DMR-1644779 and the state of Florida. SW's ODNP team acknowledges grant support from NSF (CHEM-2203405). LF holds the Bertha and Isadore Gudelsky Professorial Chair and Heads the Clore Institute for High-Field Magnetic Resonance Imaging and Spectroscopy at the Weizmann Institute; their support, as well as that of the Perlman Family Foundation, is acknowledged.

References

- [1] A.W. Overhauser, Polarization of Nuclei in Metals, Phys. Rev. 92 (2) (1953) 411–415.
- [2] T. Carver, Experimental Verification of the Overhauser Nuclear Polarization Effect, Phys. Rev. 102 (1956) 975–981.
- [3] L.R. Becerra, G.J. Gerfen, R.J. Temkin, D.J. Singel, R.G. Griffin, Dynamic nuclear polarization with a cyclotron resonance maser at 5 T, Phys. Rev. Lett. 71 (21) (1993) 3561–3564.
- [4] Maly, T.; Debelouchina, G. T.; Bajaj, V. S.; Hu, K.-N.; Joo, C., -G.; Mak Jurkauskas, M. L.; Sirigiri, J. R.; van der Wel, P. C. A.; Herzfeld, J.; Temkin, R. J.; Griffin, R. G., Dynamic nuclear polarization at high magnetic fields. J. Chem. Phys. 2008, 128, 052211.
- [5] Q.Z. Ni, E. Daviso, T.V. Can, E. Markhasin, S.K. Jawla, T.M. Swager, R.J. Temkin, J. Herzfeld, R.G. Griffin, High Frequency Dynamic Nuclear Polarization, Accounts Chem. Res. 46 (9) (2012) 1933–1941.

- [6] U. Akbey, W.T. Franks, A. Linden, S. Lange, R.G. Griffin, B.-J. Rossum, H. Oschkinat, Dynamic Nuclear Polarization of Deuterated Proteins, Angew. Chem. Int. Ed. 49 (2010) 7803–7806.
- [7] J.H. Ardenkjaer-Larsen, F. Fridlund, A. Gram, G. Hansson, L. Hansson, M.H. Lerche, R. Servin, M. Thaning, K. Golman, Increase in signal-to-noise ratio of > 10,000 times in liquid-state NMR, Proc. Natl. Acad. Sci. USA 100 (2003) 10158– 10163
- [8] K.M. Brindle, S.E. Bohndiek, F.A. Gallagher, M.I. Kettunen, Tumor imaging using hyperpolarized ¹³C magnetic resonance spectroscopy, Magn. Reson. Med. 66 (2011) 505–519.
- [9] S.J. Nelson, D. Vigneron, J. Kurhanewicz, A. Chen, R. Bok, R. Hurd, DNP-Hyperpolarized ¹³C Magnetic Resonance Metabolic Imaging for Cancer Applications, Appl. Magn. Reson. 34 (2008) 533–544.
- [10] J. Kurhanewicz, D.B. Vigneron, K. Brindle, E.Y. Chekmenev, A. Comment, C.H. Cunningham, R.J. DeBerardinis, G.G. Green, M.O. Leach, S.S. Rajan, R.R. Rizi, B.D. Ross, W.S. Warren, C.R. Malloy, Analysis of Cancer Metabolism by Imaging Hyperpolarized Nuclei: Prospects for Translation to Clinical Research, Neoplasia 13 (2011) 81–97.
- [11] T. Harris, C. Bretschneider, L. Frydman, Dissolution DNP NMR with solvent mixtures: Substrate concentration and radical extraction, J. Magn. Reson. 211 (2011) 96–100.
- [12] A. Bornet, R. Melzi, A.J.P. Linde, P. Hautle, B. van den Brandt, S. Jannin, G. Bodenhausen, Boosting Dissolution Dynamic Nuclear Polarization by Cross Polarization, Phys. Chem. Lett. 4 (2013) 111–114.
- [13] S. Bowen, C. Hilty, Rapid sample injection for hyperpolarized NMR spectroscopy, Phys. Chem. Chem. Phys. 12 (2010) 5766–5770.
- [14] A. Abragam, Overhauser Effect in Nonmetals, Phys. Rev. 98 (6) (1955) 1729–1735.
- [15] I. Solomon, Relaxation Processes in a System of Two Spins, Phys. Rev. 99 (1955) 559–565.
- [16] M.-T. Turke, M. Bennati, Comparison of Overhauser DNP at 0.34 and 3.4 T with Frémy's Salt, Appl. Magn. Reson. 43 (2012) 129–138.
- [17] T. Orlando, R. Dervisoğlu, M. Levien, I. Tkach, T.F. Prisner, L.B. Andreas, V.P. Denysenkov, M. Bennati, Dynamic Nuclear Polarization of ¹³C Nuclei in the Liquid State over a 10 Tesla Field Range, Angew. Chem. Int. Ed. 58 (5) (2019) 1402–1406.
- [18] V.P. Denysenkov, T.F. Prisner, Liquid-State Overhauser DNP at High Magnetic Fields, eMagRes 8 (1) (2019) 14.
- [19] S. van Meerten, High Sensitivity NMR in a Microfluidic Context, Radboud University, 2020.
- [20] N.M. Loening, M. Rosay, V. Weis, R.G. Griffin, Solution-State Dynamic Nuclear Polarization at High Magnetic Field, J. Am. Chem. Soc. 124 (30) (2002) 8808– 8800
- [21] D. Yoon, A.I. Dimitriadis, M. Soundararajan, C. Caspers, J. Genoud, S. Alberti, E. de Rijk, J.-P. Ansermet, High-Field Liquid-State Dynamic Nuclear Polarization in Microliter Samples, Anal. Chem. 90 (9) (2018) 5620–5626.
- [22] V. Weis, M. Bennati, M. Rosay, J.A. Bryant, R.G. Griffin, High-Field DNP and ENDOR with a Novel Multiple-Frequency Resonance Structure, J. Magn. Reson. 140 (1999) 293–299.
- [23] D. Dai, X. Wang, Y. Liu, X.-L. Yang, C. Glaubitz, V. Denysenkov, X. He, T.F. Prisner, J. Mao, Room-temperature dynamic nuclear polarization enhanced NMR spectroscopy of small biological molecules in water, Nat. Commun. 12 (2021) 6880.
- [24] T. Dubroca, S. Wi, J. van Tol, L. Frydman, S. Hill, Large volume liquid state scalar Overhauser dynamic nuclear polarization at high magnetic field, Phys. Chem. Chem. Phys. 21 (2019) 21200–21204.
- [25] C. Griesinger, M. Bennati, H.M. Vieth, C. Luchinat, G. Parigi, P. Höfer, F. Engelke, S.J. Glaser, V. Denysenkov, T.F. Prisner, Dynamic nuclear polarization at high magnetic fields in liquids, Prog. Nucl. Magn. Reson. Spectrosc. 64 (2012) 4–28.
- [26] Wang, X.; Isley III, W. C.; Salido, S. I.; Sun, Z.; SOng, L.; Tsai, K. H.; Cramer, C. J.; Dorn, H. C., Optimization and prediction of the electron–nuclear dipolar and scalar interaction in ¹H and ¹³C liquid state dynamic nuclear polarization. Chem. Sci. 2015, 6, 6482-6495.
- [27] Dubroca, T.; Smith, A. N.; Pike, K., J.; Froud, S.; Wylde, R.; Trociewitz, B.; McKay, J.; Mentink-Vigier, F.; J., v. T.; Wi, S.; Brey, W.; Long, J. R.; Frydman, L.; Hill, S., A quasi-optical and corrugated waveguide microwave transmission system for simultaneous dynamic nuclear polarization NMR on two separate 14.1 T spectrometers. J. Magn. Reson. 2018, 289, 35-44.
- [28] M. Bennati, C. Luchinat, G. Parigi, M.-T. Turke, Water ¹H relaxation dispersion analysis on a nitroxide radical provides information on the maximal signal enhancement in Overhauser dynamic nuclear polarization experiments, Phys. Chem. Chem. Phys. 12 (2010) 5902–5910.
- [29] G. Liu, M. Levien, N. Karschin, G. Parigi, C. Luchinat, M. Bennati, One-thousand-fold enhancement of high field liquid nuclear magnetic resonance signals at room temperature, Nat. Chem. 9 (2017) 676–680.
- [30] G. Parigi, E. Ravera, M. Bennati, C. Luchinat, Understanding Overhauser Dynamic Nuclear Polarisation through NMR relaxometry, Mol. Phys. 117 (2019) 888–897.
- [31] T. Prisner, V. Denysenkov, D. Sezer, Liquid state DNP at high magnetic fields: Instrumentation, experimental results and atomistic modelling by molecular dynamics simulations, J. Magn. Reson. 264 (2016) 68–77.
- [32] M. Mishkovsky, L. Frydman, Progress in Hyperpolarized Ultrafast 2D NMR Spectroscopy, ChemPhysChem 9 (2008) 2340–2348.
- [33] R. Sarkar, A. Comment, P.R. Vasos, S. Jannin, R. Gruetter, G. Bodenhausen, H. Hall, D. Kirik, V.P. Denisov, Proton NMR of 15N-Choline Metabolites Enhanced by Dynamic Nuclear Polarization, J. Am. Chem. Soc. 131 (2009) 16014–16015.

- [34] T. Harris, P. Giraudeau, L. Frydman, Kinetics from Indirectly Detected Hyperpolarized NMR Spectroscopy by Using Spatially Selective Coherence Transfers, Chem. Eur. J. 17 (2) (2011) 697–703.
- [35] J. Wang, F. Kreis, A.J. Wright, R.L. Hesketh, M.H. Levitt, K.M. Brindle, Dynamic 1 H imaging of hyperpolarized [1-13 C]lactate in vivo using a reverse INEPT experiment, Magn. Reson. Med. 79 (2) (2018) 741–747.
- [36] L. Frydman, D. Blazina, Ultrafast two-dimensional nuclear magnetic resonance spectroscopy of hyperpolarized solutions, Nature Phys 3 (2007) 415–419.
- [37] E.Y. Chekmenev, V.A. Norton, D.P. Weitekamp, P. Bhattacharya, Hyperpolarized ¹H NMR Employing Low γ Nucleus for Spin Polarization Storage, J. Am. Chem. Soc. 131 (9) (2009) 3164–3165.
- [38] P. Dzien, A. Fages, G. Jona, K.M. Brindle, M. Schwaiger, L. Frydman, Following Metabolism in Living Microorganisms by Hyperpolarized H-1 NMR, J. Am. Chem. Soc. 138 (37) (2016) 12278–12286.
- [39] G.A. Morris, R. Freeman, Enhancement of nuclear magnetic resonance signals by polarization transfer, J. Am. Chem. Soc. 101 (3) (1979) 760–762.
- [40] D.P. Burum, R.R. Ernst, Net polarization transfer via a J-ordered state for signal enhancement of low-sensitivity nuclei, J. Magn. Reson. 39 (1980) 163–168.
- [41] S. Braun, H.-O. Kalinowski, S. Berger, 150 and More Basic NMR Experiments: A Practical Course, Weinheim, Germany, WILEY-VCH, 1998.
- [42] Dubroca, T.; Scott, K.; Soundararajan, M.; McKay, J.; Trociewitz, B.; Hill, S.; van Tol, H.; Wi, S.; Frydman, L., High Efficiency Liquid Overhauser DNP Probe at 14.1 T. **2021**, Manuscript in preparation.

- [43] X. Wang, W.C. Isley III, S.I. Salido, Z. Sun, L. Song, K.H. Tsai, C.J. Cramer, H.C. Dorn, Optimization and prediction of the electron-nuclear dipolar and scalar interaction in ¹H and ¹³C liquid state dynamic nuclear polarization, Chem. Sci. 6 (2015) 6482–6495.
- [44] T. Orlando, R. Dervişoğlu, M. Levien, I. Tkach, T.F. Prisner, L.B. Andreas, V.P. Denysenkov, M. Bennati, Dynamic nuclear polarization of C-13 nuclei in the liquid state over a 10 Tesla field range, Angew. Chem. Int. Ed. 58 (2019) 1402–1406.
- [45] M. Levien, M. Hiller, I. Tkach, M. Bennati, T. Orlando, Nitroxide Derivatives for Dynamic Nuclear Polarization in Liquids: The Role of Rotational Diffusion, J. Phys. Chem. Lett. 11 (5) (2020) 1629–1635.
- [46] A.J. Shaka, J. Keeler, T. Frenkiel, R. Freeman, An Improved Sequence for Broadband Decoupling: WALTZ-16, J. Magn. Reson. 52 (1983) 335–338.
- [47] C. Szántay, Analysis and Implications of Transition-Band Signals in High-Resolution NMR, J. Magn. Reson. 135 (1998) 334–352.
- [48] D. Neuhaus, M.P. Williamson, The Nuclear Overhauser Effect in Structural and Conformational Analysis, VCH Publishers Inc, New York, 1989.
- [49] M.S. Morales-Rios, P. Joseph-Nathan, NMR Studies of Indoles and Their N-Carboalkoxy Derivatives, Magn. Reson. Chem. 25 (1987) 911–918.
- [50] Y. Rao, A. Venkatesh, P. Moutzouri, L. Emsley, ¹H Hyperpolarization of Solutions by Overhauser Dynamic Nuclear Polarization with ¹³C-¹H Polarization Transfer, J. Phys. Chem. Lett. 13 (2022) 7749–7755.